

Physical properties of marine boundary layer aerosol particles of the mid-Pacific in relation to sources and meteorological transport

D. S. Covert

Department of Atmospheric Sciences, University of Washington, Seattle

V. N. Kapustin

Joint Institute for the Study of the Atmosphere and Ocean, University of Washington, Seattle

T. S. Bates and P. K. Quinn

NOAA, Pacific Marine Environmental Laboratory, Seattle

Abstract. Aerosol measurements were made on three cruises in the mid-Pacific along longitude 140°W from 55°N to 70°S for a total of about 90 days in 1992 and 1993. The three data sets document the aerosol concentration and general features of its number-size distribution in the marine boundary layer (MBL) and their variation with latitude and meteorological conditions. Mean concentration varied from 300 cm⁻³ in the tropics to 500 cm⁻³ in the midlatitudes outside of continental air masses. Infrequent short-term spikes in concentration ranged up to 2000 cm⁻³. Two dominant modes were observed, the Aitken and accumulation, with mean diameters of 25 to 60 nm and 150 to 200 nm, respectively. An intermittent ultrafine mode was noted at diameters less than 25 nm. The concentration and dominance of one mode over another depended on the relative strength of the entrainment of ultrafine and Aitken particles from the free troposphere (FT) into the MBL compared to the rate of growth of Aitken mode into accumulation mode particles and removal rate of the accumulation mode. In general, aging times were shorter in the subtropics, longer in the tropics, and variable in the midlatitudes. The rate of new particle formation within the MBL itself was either low and did not contribute significantly to the observed number concentration or, if the rate was high, it occurred infrequently and was not observed in these experiments.

Introduction

Aerosol number-size distribution in the marine boundary layer (MBL) and free troposphere (FT) over the mid-Pacific has been studied to the point where a general description of its structure and spatial variability can be made. On the basis of measurements in the Antarctic coastal regions [Ito, 1989], a general conceptual model of a multimodal number distribution in the high- and mid-latitudes of the southern Pacific was formulated [Ito, 1993] which employed both aerosol dynamics and atmospheric dynamics to explain particle formation, evolution, and transport. Aerosol measurements made at the surface and in the stratus and stratocumulus clouds of the MBL have identified some of the fundamental cloud and gas-to-particle conversion processes that control particle number-size distribution [Hoppel and Frick, 1990; Hegg et al., 1992; Quinn et al., 1993; Hoppel et al., 1994]. These processes explain to a large degree the bimodal number-size distribution ubiquitously observed in the remote MBL with concentration maxima at about 50 and 200 nm diameter and a minimum between these

sizes. A large-scale numerical model of aerosol nucleation and dynamics in the FT and MBL [Raes et al., 1993; Raes, 1995] has provided a general understanding of the particle concentration and number distribution that result from gas-to-particle conversion in the marine atmosphere. In particular, the results demonstrate sensitivity to controlling processes and a low probability of particle nucleation in the MBL, implying that injection by mixing with the FT is a major source of new submicrometric particles in the MBL. However, a smaller-scale model of sulfuric acid nucleation in the MBL [Kerminen and Wexler, 1995] shows that the particle formation rate associated with vertical motions may be high during noncloudy periods. Measurements in the FT of the equatorial Pacific [Clarke, 1993] showed that nucleation in the upper troposphere and subsequent growth by coagulation and vapor diffusion could be a major source of new particles in that region, and provide support for the modeling results of F. Raes.

From these previous results a general picture of the source and evolution of the MBL aerosol away from continental sources can be constructed. A probable major source of new submicrometric MBL aerosol on a number basis is subsidence and mixing from the FT with small contributions by sea salt. The source of supermicrometric aerosol is mainly sea salt with some transport of mineral dust. These particles are transformed through coagulation, diffusional deposition of vapors, and cloud

Copyright 1996 by the American Geophysical Union.

Paper number 95JD03068.
0148-0227/96/95JD-03068\$05.00

droplet nucleation. New mass accumulates on aerosol particles by diffusional growth and cloud processing, mainly in the size range above 60 nm. These processes result in a multimodal aerosol with stable number modes at mean diameters around 50 and 200 nm and a more variable mode around 25 nm or less. Mass modes occur at about 250 to 300 nm and 2 to 5 μm .

Within this context we present and interpret the results of extensive submicrometric aerosol number-size distribution measurements during three research cruises in the mid-Pacific along 140°W longitude from 55°N to 70°S latitude, made in concert with gas and aerosol chemistry measurements and aerosol optical measurements. The cruises were named after the geophysical programs and years of which they were part: Marine Aerosol and Gas Exchange (MAGE 92) and Radiatively Important Trace Species (RITS 93 and RITS 94). The MAGE 92 cruise began in Los Angeles, California, in February of 1992 and ended there in March of 1992 after transects to Nuku Hiva in the French Marquesas Islands. RITS 93 began in Punta Arenas, Chile, in March of 1993 and ended in Seattle, Washington, in May of 1993. RITS 94 began in Seattle in November of 1993 and ended in Punta Arenas in January of 1994. The cruise tracks, time points along the tracks, and the location and date of extended sampling stations are illustrated in Figure 1.

The main goal of the aerosol physical experiments on these cruises was to document MBL aerosol number-size distribution in detail over a broader range of latitude, time of year, and weather conditions than had been done previously and thereby to derive a data set that could be used to test models of MBL aerosol dynamics. Another goal was to compare the physical data to other gas and particulate phase parameters such as dimethylsulfide (DMS), SO_2 , NH_3 , and size-resolved aerosol mass and ionic composition. A further goal was to derive a qualitative regional mapping of the source and age of particles in the MBL from analysis of the aerosol and meteorological data. Particulate source can be thought of in two ways that must be considered separately. New particles, which increase total number concentration in the MBL, can be formed by nucleation from gaseous precursors or can be mixed from adjacent layers. New particulate mass can be added this way as well, but the majority of new mass accumulates on existing particles by vapor condensation and cloud oxidation processes and does not increase the number concentration. Particulate age is not strictly a time, for example, residence time, but rather a change in particles dependent on parameters such as coagulation, condensational growth, and cloud processing.

A more extensive presentation of aerosol chemistry and

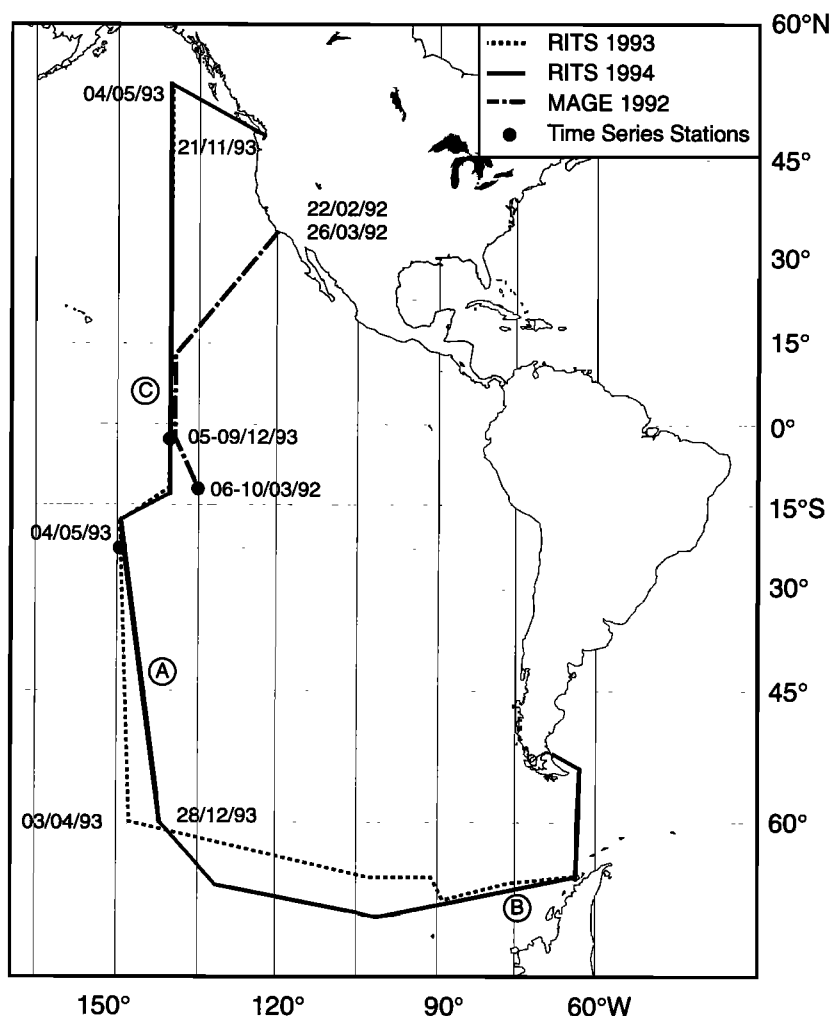


Figure 1. Ship's cruise tracks for Marine Aerosol and Gas Experiment, MAGE 92, and Radiatively Important Trace Species, RITS 93 and RITS 94, cruises. Letters refer to locations of aerosol number-size distributions plotted in Figure 7.

optical data may be found in work by Quinn *et al.* [1995]. A description and summary of DMS measurements from the Pacific can be found in work by Bates *et al.* [1993] and Yvon *et al.* [1995].

Experimental Methods

Particle number concentration was measured continuously with two condensation particle counters (UCPC model 3025 and CPC model 3760, TSI Inc., St. Paul, Minn.) which determined the concentration, n , of particles with diameters, D_p , greater than 3 nm and 14 nm, $n(>3)$ and $n(>14)$, respectively. The difference between these two is taken as a measure of the concentration of ultrafine aerosol, although the increment does not correspond necessarily to the ultrafine mode. The number-size distribution of the particles was measured every 10 min with a differential mobility particle sizer (DMPS) covering the range 20 to 600 nm. The mobility distribution from the DMPS was inverted to a number distribution by assuming that a Fuchs-Boltzman charge distribution resulted from the Kr^{85} charge neutralizer (model 3077, TSI Inc.). All size data were converted to a differential format, $dn/d\log D_p$.

Local weather and chemistry data, including surface temperature, dew point temperature, wind speed and direction, rawinsonde data, ozone and dimethylsulfide concentrations, and particulate chemical compositions, were collected on the cruises and used in the interpretation of the aerosol physical data. Rawinsonde balloons were launched at standard 12-hour intervals and the profiles were analyzed for inversion height and the depth of the mixed layer. The hybrid single-particle Lagrangian integrated trajectory model (HY-SPLIT, Draxler [1992]) was used to calculate air mass back trajectories based on wind fields from the medium range forecast model every 12 hours for the duration of the experiments. The starting point for each trajectory was the ship's position and 950-mbar elevation. The 900-mbar surface was the average height of the MBL based on analysis of shipboard rawinsonde data. We estimated the MBL residence time of an air parcel and the aerosol it contained from the length of time it had spent below 900 mbar in the MBL prior to its measurement on the ship as determined by the calculated trajectories. Maps of surface and upper air meteorology and satellite images of cloud cover were obtained from the National Weather Service archives.

Results and Discussion

The aerosol physical data were largely consistent among the three cruises. Thus the focus of the interpretation here will be on the general features in conjunction with latitude, regional-scale meteorology, and air mass trajectories, along with specific illustrative and representative examples. Particular analysis is made for the South Pacific, where synoptic conditions were relatively similar during the three experiments as determined by the trajectories, by the surface and upper air weather maps, and by comparison to a climatological study of southern hemispheric air motions and synoptic climate [Wendland and McDonald, 1986; Salinger *et al.*, 1995].

A wide range of atmospheric conditions was observed, including unpolluted marine air in the remote South Pacific from 70°S to tropical latitudes, and a mixture of marine and continental air masses in the North Pacific, particularly off the coast of southern California. The observations included meteorological conditions that ranged from stable cloud-topped marine boundary layers, to cyclonic and anticyclonic systems and frontal

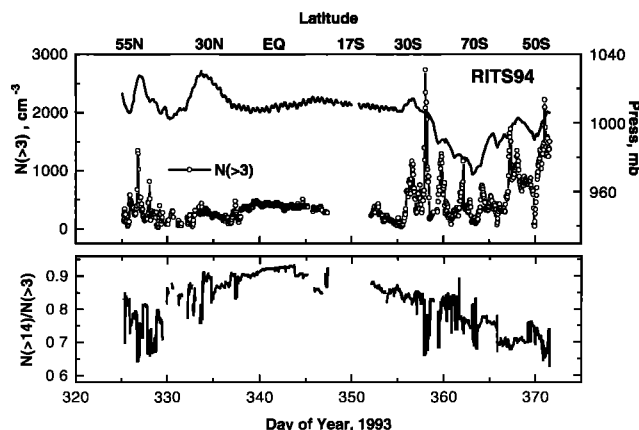


Figure 2. Particle number concentration data versus latitude and time for RITS 94. (a) Total number concentration greater than 3 nm, $n(>3)$, and sea level pressure. (b) Ratio of accumulation plus Aitken mode number concentration to total particle concentration, $n(>14)/n(>3)$.

passages in the midlatitudes, to deep convection in the Intertropical Convergence Zone (ITCZ). As expected, a wide range of particle concentrations and number-size distributions was observed. However, a general pattern associated with large-scale meteorological features was clear in the data from each cruise, and the pattern was strengthened by the multiyear data set.

Figure 2 presents the total particulate number concentration, $n(>3)$, as a function of time and latitude for the RITS 94 cruise. Also shown is sea level pressure, indicating the variability associated with latitudinal and regional scale cyclonic systems. The time series data from RITS 93 and MAGE 92 were similar but less continuous. The number concentration in the tropics and subtropics from 35°S to 35°N was between 150 and 400 cm^{-3} and averaged 280 cm^{-3} (s.d. ± 50). In the mid-latitudes of both hemispheres (35° to 65°) minimum values were again about 150 cm^{-3} , but the mean concentration was 500 cm^{-3} (s.d. ± 100). Maximum values occurred in short-duration spikes ranging from 1000 to 2000 cm^{-3} . The ratio of $n(>14)/n(>3)$ is presented in the lower panel of Figure 2 to show that when such a normalization is performed much of the mesoscale variability is removed, resulting in a relatively smooth curve that varies from 0.9 in the tropics to 0.7 in the northern and southern midlatitudes. This illustrates the relative dominance of larger particles in the tropical regions.

Examples of the number-size distribution, $dn/d\log D_p$, from widely separate times and latitudes during RITS 93 and RITS 94 are presented in Figures 3a–3e. These distributions, which encompass 6 to 24 hours of data each, were selected to illustrate distinct types of distributions associated with different meteorological conditions, aerosol sources, and aging processes. In spite of the variability in number concentration there are general features common to each. There is a local maximum or mode in the number concentration between 150 and 250 nm diameter, a minimum between 60 and 100 nm, and a second local maximum (or inflection) between 30 and 60 nm. The two modes are termed the accumulation and Aitken modes, respectively. These features persist in the larger data set even though there is wide variation in both total concentration and the ratio of modal concentrations. A more transient feature is a concentration mode below 25 nm, termed the ultrafine mode. The distributions are classified as bimodal (closed), open, or semi-open, depending on the shape of the Aitken mode at diameters less than 25 nm.

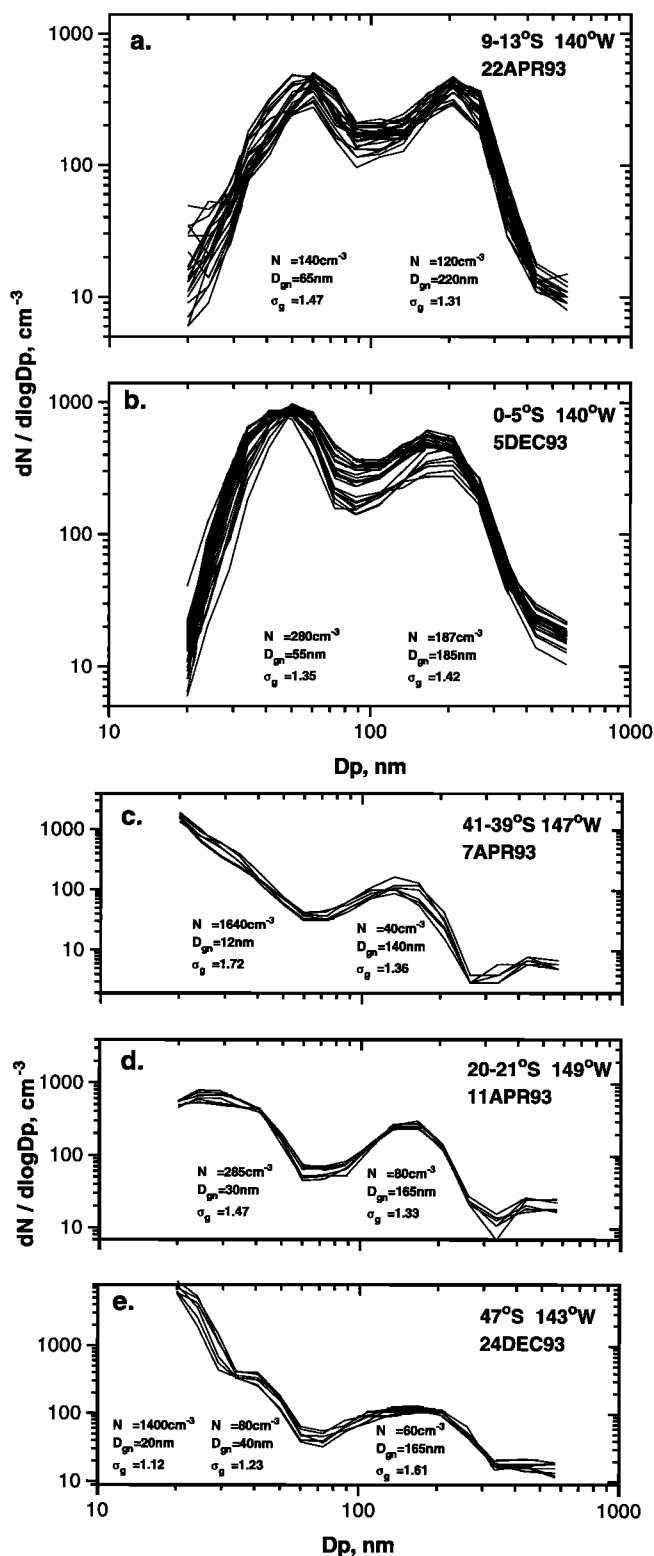
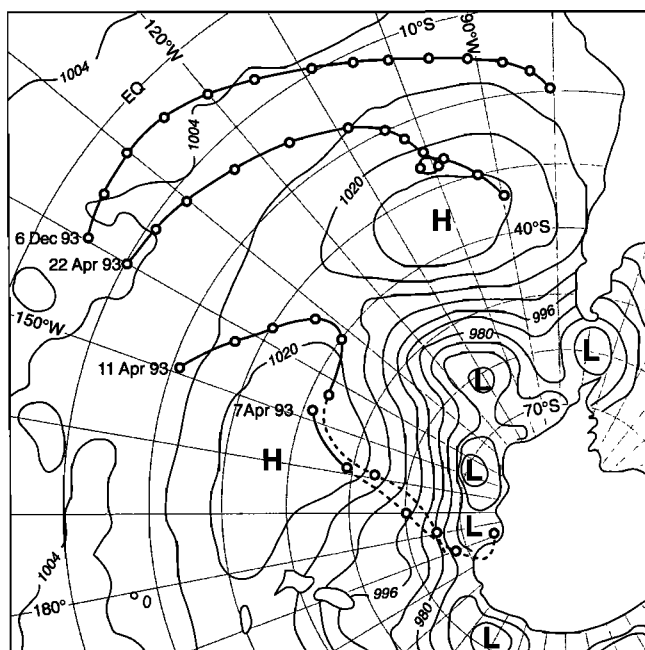


Figure 3. Particle number-size distribution, $dn/d\log D_p$, for five times and locations during RITS 93 and RITS 94, illustrating types of distributions observed under different but repeatedly observed conditions of meteorology, aerosol sources, and aging processes. Each line represents the average over 60 min; each plot represents 24 or 6 hours of data. The mean number concentration, number mean geometric diameter, and standard deviation of the averaged data determined by a lognormal fit to the modes are given: (a) RITS 93, tropical, bimodal distribution; (b) RITS 94, tropical, bimodal distribution; (c) RITS 93, midlatitude, open distribution; (d) RITS 93, tropical, semi-open distribution; and (e) RITS 94, midlatitude, open distribution.



distribution was associated with either large-scale subsidence or post-frontal subsidence and advection of anticyclonic systems. Trajectory analysis of these situations indicates the air mass had a residence time of 5 days or less in the MBL.

Three-dimensional trajectories for the specific cases corresponding to the number distributions of Figure 3a and 3b (tropical, bimodal) and 3c and 3d (midlatitude, open evolving to subtropical, semi-open) are illustrated as two-dimensional projections on a surface weather map in Figure 4. This map corresponds specifically to the date and time of the number distributions in Figure 3c but is very similar to those for all four dates and trajectories. In Figure 5 three-dimensional plots of two of these trajectories (corresponding to Figures 3b and 3c) are presented.

The steeply subsiding trajectory in Figure 5 that terminated at the ship's location and 950 mbar on April 7, 1993, was associated with the open number-size distribution dominated by Aitken and ultrafine mode aerosol shown in Figure 3c. On the surface weather map, the time spent in the MBL after subsiding from the FT to below 900 mbar, as indicated by the solid line, was less than 1 day. The subsidence was associated with a frontal passage followed by advection of an anticyclonic system from the west. Four days later and 20° further north, the trajectory for the ship's location indicated that the air had spent 4 to 5 days in the MBL after subsiding. The distribution at the end of this trajectory (Figure 3d) had a much reduced concentration of particles less than 30 nm diameter, a defined Aitken mode maximum, and a greater concentration and larger modal size in the accumulation range, all indicative of aging by coagulation, condensation, and cloud processing.

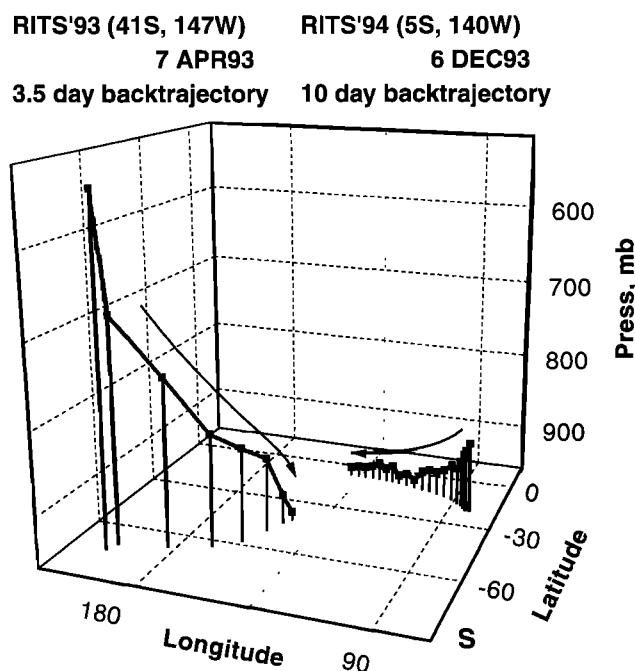


Figure 5. Three-dimensional trajectory plots for two times during RITS 93 and RITS 94 cruises corresponding to number-size distributions in Figures 3b and 3c. Points are plotted every 12 hours back in time for 3.5 days in RITS 93 and 10 days in RITS 94. The latter represents a case when the air had a residence time of 7 days or more in the MBL following its subsidence from the FT and prior to its arrival at the ship's position. The contrasting case, during RITS 93, followed a subsidence event when the MBL residence time was less than 1 day.

The trajectory shown in Figure 5 that terminated at the ship's position on December 6, 1993 (corresponding to the tropical, well-aged, bimodal distribution of Figure 3b), was confined to the MBL for more than 5 days. The surface projection of this and the similar trajectory for April 22, 1993, 5° further south (corresponding to the tropical distribution of Figure 3a), are shown on the map in Figure 4. The trajectories are similar in their MBL residence times of 5 days or more because they are associated with large-scale flow around similar high pressure regions, but they originate at different latitudes and are associated with different cloud conditions along their paths. The general modal features of both distributions are the same, but the mean diameters and concentrations of the Aitken and accumulation modes differ slightly, probably due to differing chemical and cloud physics parameters that cannot be quantified along the trajectory paths.

One of the goals of this study was to qualitatively assess the relative age of the aerosol by analysis of the number-size distribution. This age is dependent not just on time but also on processes such as coagulation, condensational growth, and cloud droplet nucleation and growth, and thus is a function of temperature, humidity, and concentration of condensable and water-soluble gas phase species. The difference between the particle concentrations at 50 and 20 nm, $dn(50)/d\log D_p - dn(20)/d\log D_p$, abbreviated n^* , was calculated from the number-size distribution as a parameter related to the relative age of the aerosol. The concentration at 50 nm was selected for comparison because it was relatively stable, not subject to rapid changes due to removal by clouds and precipitation or to production by new particle nucleation and condensational growth. Negative values are indicative of an aerosol that has a dominant ultrafine mode or an Aitken mode with a mean diameter smaller than about 40 nm and thus has had a relatively shorter aging time in the MBL, on the order of a few days or less. Positive values are indicative of an aerosol that has had a longer aging time of several days or more and has been relatively isolated from sources of new particles. Obviously, any value is possible, and small differences cannot be clearly interpreted. For the RITS 93 data, n^* is plotted versus latitude in Figure 6a along with the time series of sea level pressure. There is appreciable variability in n^* but there are extensive latitude bands where the parameter is either near zero, or predominantly positive or negative. A smoothed composite plot of n^* for all three cruises is presented in Figure 6b. Again, there is variability due to specific synoptic meteorological events during the three cruises but there is also an obvious envelope of n^* values versus latitude that is consistent over the three cruises. In the tropical region from about 20°S to 15°N the values are positive. In the regions further north and south to about 30°N and 40°S the values are generally negative. Further poleward, the values are either near zero or vary positively or negatively in response to cyclonic meteorology and air chemistry. The value of n^* is also strongly negative in the air mass from the North American continent (RITS 93, 20°N to 30°N, Figure 6b). Thus the aerosol with the consistently greatest age was observed in the tropical latitudes; that with the consistently shortest age was in the latitude bands 20° north and south of the tropical region.

Time series of the 10-min time-resolved number distribution data provide a means to assess mesoscale variation of the aerosol and to identify major changes and specific events. This can be illustrated with plots of number-size distribution versus time, $dn(D_p, t)/d\log D_p$, either as a three-dimensional surface, as shown in Figure 7, or as a contour plot where concentration is represented by the contour variable, as shown in Figure 8. For

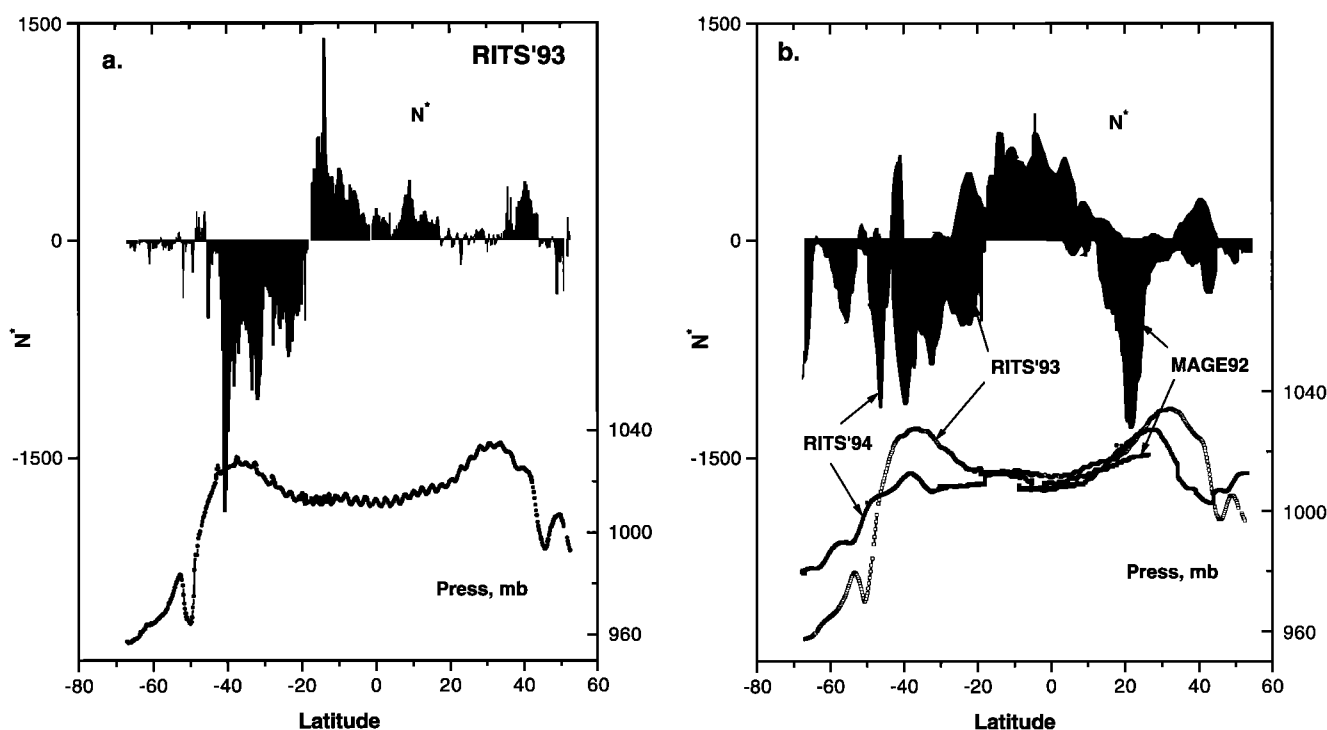


Figure 6. Latitudinal cross section-plots of n^* , the difference in the particle concentration at 50 and 20 nm, $dn(50)/d\log D_p - dn(20)/d\log D_p$. A positive value of n^* indicates that the Aitken mode is dominated by relatively larger and more-aged aerosol; a negative value is indicative of smaller less-aged aerosol. Sea level pressure, plotted on the same graph as an indicator of the synoptic-scale weather regimes, shows low pressure in the tropics (with diurnal cycles), high pressure around 40°S and 30°N , and the cyclonic high and low passages around 55°S and 50°N . (a) RITS 93 cruise without time or latitudinal smoothing, showing the hourly and longer time variation. (b) MAGE 92, RITS 93 and RITS 94. The data have been smoothed by a 4-hour running mean to highlight regional-scale meteorology and latitudinal trends. In tropical regions the mode of the number-size distribution in the Aitken range was centered near 50 nm, while in the subtropics and midlatitudes the Aitken mode was generally shifted to smaller sizes or was “open,” that is, was not a closed mode or was a shoulder on an ultrafine number mode. The larger variability in this parameter in the southern hemisphere from 40°S to 70°S during RITS 94 is due to passage of cyclonic systems and fronts.

specific events three-dimensional plots are very graphic and clear; however, a longer time series of data presented as a three-dimensional surface suffers from loss of perspective when viewed from only one angle, and is clearer in a contour plot. The three-dimensional plots of number distribution versus time or latitude in Figure 7 present three relatively short time periods (1.5 to 7 days) which illustrate both stability and dramatic change in the aerosol.

Figure 7a shows data from December 3 to 4, 1993, during RITS 94, covering the tropical region of the cruise starting at 8°N and moving to 3°N . There are three distinct distributions within this time period. A bimodal, tropical distribution is evident early and late in the period, with roughly equal numbers in the Aitken and accumulation modes, similar to Figures 3a and 3b. However, there was a much lower concentration south of the ITCZ during the latter part of the period. A distribution dominated by an Aitken mode at relatively small size and high concentration was observed for about 6 hours in the middle of the period. This event corresponded to the passage of the ITCZ when the ship was in the vicinity of deep cumulus convection and rain showers. We hypothesize that this Aitken mode is the result of mesoscale subsidence from the FT associated with these cumulus cells but we could find no supporting evidence through tracers (O_3 or water vapor) of air from aloft.

Figure 7b illustrates a period of 7 days in austral autumn during RITS 93 over a wide latitude band from 45°S to 20°S when the aerosol concentration was consistently dominated by a small diameter Aitken mode. This series includes the data in Figure 3d. The accumulation mode was always present as a separate but minor mode. This corresponds to the period illustrated in Figure 6a when n^* was consistently negative and the ship was passing through a region of high pressure and subsiding air. Clouds and precipitation were minimal during this period.

Figure 7c illustrates a 4-day period during RITS 94 in the Southern Ocean (62° to 69°S) when there was considerable change in the distribution related to meteorological variability on a scale of hours. The accumulation mode was always present and the modal size was between 150 and 200 nm. The Aitken mode was generally dominant in terms of number but concentration was highly variable, and on one several-hour occasion (about day 2) it was overwhelmed by a high concentration of particles in the ultrafine mode. This was related to a frontal passage and subsidence, as indicated by surface pressure patterns and air mass trajectories on that date. The number distribution in this MBL region is the result of multiple processes of transport, condensational growth, cloud processing, and removal which were not quantified. With a more pro-

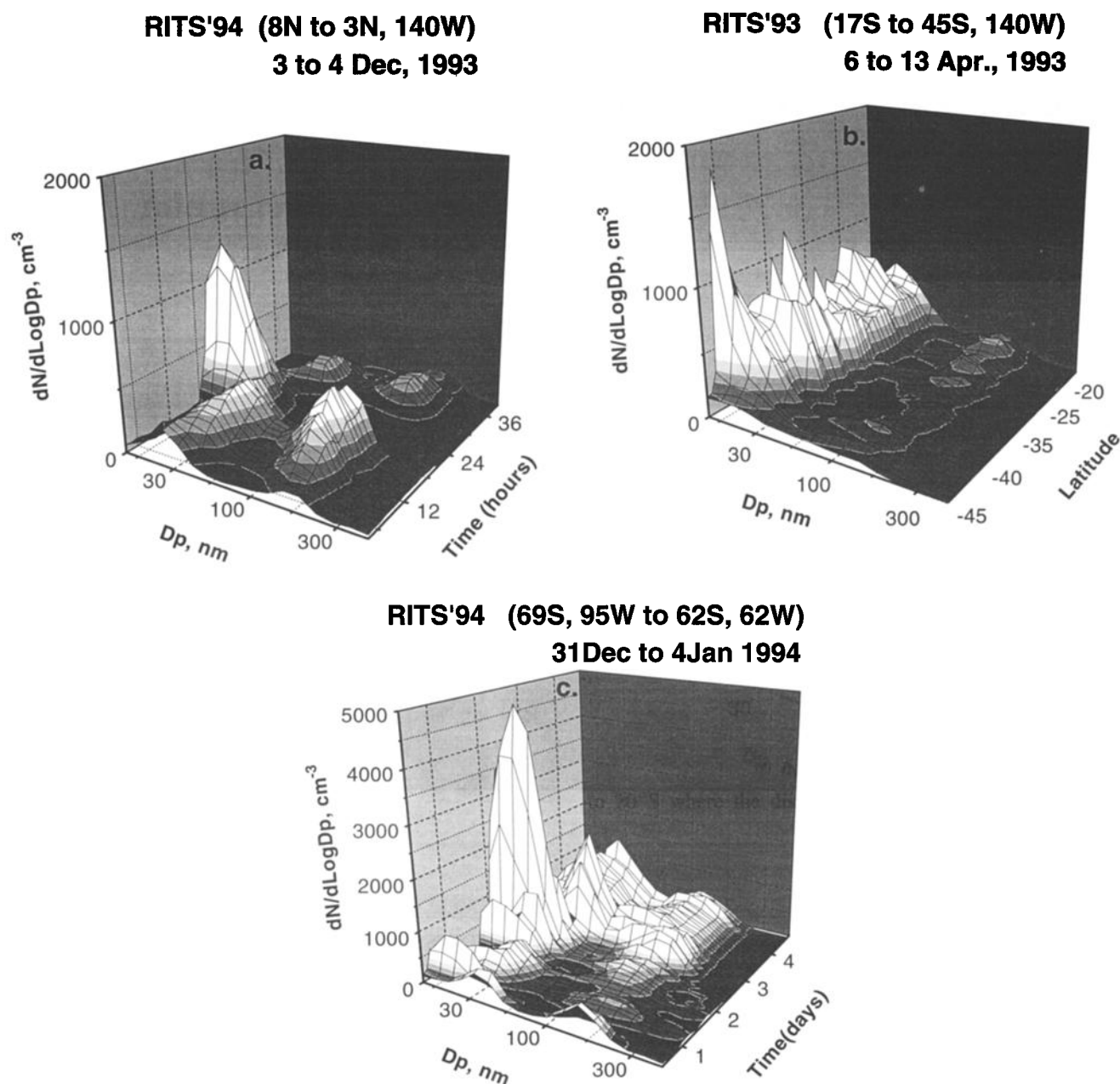


Figure 7. Three-dimensional plots of number-size distribution, $dn/d\log D_p$, versus D_p versus time or latitude. The shaded portion of the scale on the concentration axis is the same in all three plots, 0 to 500 particles cm^{-3} , but the maximum on the concentration scale varies. (a) Time series from the tropics, 7°N 140°W , December 3 to 4, 1993, during RITS 94. The Aitken mode with high concentrations and relatively small modal diameter during the middle of the period is consistent with mesoscale subsidence from the middle or upper FT associated with vertical circulation around convective cells in the ITCZ. The bimodal distribution observed otherwise is typical of the well-aged aerosol in the tropics. (b) Latitudinal cross section in the high-pressure region of the South Pacific during RITS 93. The Aitken mode is clearly dominant. The accumulation mode is always present as a separate, if minor, mode. (c) Time series in the Southern Ocean during RITS 94. The relative concentrations of the modes shift radically depending on the location of the ship with respect to cyclonic and anticyclonic circulation and fronts.

nounced accumulation mode, the aerosol is assumed to be more aged than that depicted in Figure 7b, presumably due to growth phenomena (in and out of cloud) and longer residence times. The relatively lower accumulation mode concentration (cf. the tropical, aged distributions) is assumed to be due to more removal by precipitation.

The time series of number distributions covering the entirety of the north-south transects during the RITS 93 and RITS 94 cruises are shown in Figures 8a and 8b, respectively, as contour plots versus latitude. Three large-scale features during austral autumn are obvious in Figure 8a. First is the sequence from 40° to 20°S where the distribution is clearly dominated by the

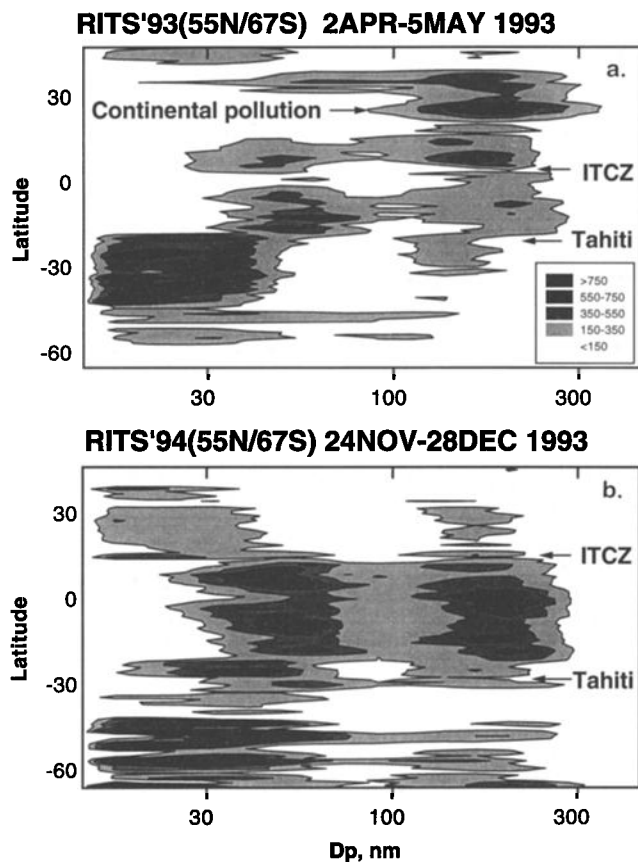


Figure 8. Contour plots of number-size distributions versus latitude for RITS 93 and RITS 94. (a) RITS 93, 55°N to 60°S. This plot again shows the dominant Aitken mode illustrated in Figure 7b from 20 to 45°S. Marked changes occur in the regions around 20°S and 25°N. A bimodal aerosol is present in the tropics and a continental accumulation mode aerosol is present around 30°N. (b) RITS 94, 55°N to 67°S. The high concentration of small Aitken particles near the ITCZ is the same event presented in Figure 7a. North and south of the ITCZ the number-size distributions exhibit Aitken and accumulation modes typical of the tropical MBL. South of the ITCZ the dominant mode shifts between the accumulation and Aitken range several times. These shifts coincided with changes in the length of time the particles spent in the MBL, with the dominant accumulation mode associated with longer residence times.

Aitken mode, as described above. Second is the tropical region north and south of the ITCZ where the distribution is bimodal with roughly equal modes. North of the ITCZ the accumulation mode dominated slightly, while south of the ITCZ the situation was reversed and the Aitken mode was the larger. Finally, in the region around 20°N there was advection of air from the North American continent with a high concentration (750 cm^{-3}) of accumulation mode aerosol, presumably from anthropogenic sources. This is in stark contrast to the lower concentration and predominantly Aitken mode aerosol observed at similar latitudes in the southern hemisphere.

Figure 8b presents data from the same region 7 months later during RITS 94, in austral late spring and early summer. The same sequence as in Figure 7a is presented, with the high-concentration Aitken mode near the ITCZ and bimodal distributions to the north and south. The tropical bimodal distribution extends over about the same latitude range as in 1993. However,

south of 5°N the dominant mode shifted twice from the Aitken to the accumulation mode and back as the ship proceeded south. Analysis of the trajectories during this time showed that these shifts were associated with a change in the length of time the air spent in the MBL after subsidence from aloft. Distributions with a more dominant accumulation mode aerosol were associated with trajectories that included 5 or more days in the MBL with a more east-to-west path, largely in the tropics. Those with a more dominant Aitken mode were associated with trajectories that included less than 5 days in the MBL and followed an anticyclonic curvature from the southeast and more subtropical latitudes. This pattern continued until about 20°S when the ship entered the region of subtropical high pressure and the aerosol number distribution shifted to dominance by a smaller diameter Aitken mode, as at similar latitudes during RITS 93.

Other parameters than residence time in the MBL, such as DMS and/or SO_2 concentration, entrainment rate from the FT, cloud cover, temperature, and humidity have been shown in model sensitivity studies to affect new particle production and the particle number distribution [Russell *et al.*, 1994; Raes, 1995]. In an effort to define causal factors for variability in the number distributions we measured, especially the ultrafine concentration, we investigated correlations between these parameters. Since the physical properties of a population of particles depend on the integral of processes acting over its lifetime, the history of these controlling parameters in time and space is needed to describe fully the aerosol measured at a given point. Lacking such sophisticated data, we have analyzed relations between point shipboard measurements of ultrafine number concentration, DMS concentration, particle surface area, ozone concentration, humidity, vertical temperature and humidity profiles, and sea level pressure.

Following the hypothesis of Raes [1993] that entrainment from the FT is the source of newly formed particles in the MBL, the relation between tracers of FT air and ultrafine particles was investigated. The clearest correlation was between ultrafine concentration and the change in dew point temperature with time. In the MBL a decrease in dew point temperature with time can be taken as an indicator of advection or subsidence of air from upper levels. The change of dew point with time depends on the initial surface dew point and on the scale of the meteorological event. To get a stable dew point parameter that is representative of synoptic scale advection changes and eliminates small scale variability, we chose to use the difference between the 6-hour and 24-hour running means, $\bar{T}_d(6) - \bar{T}_d(24)$. The 6-hour mean was selected as representative of the timescale of the variability in ultrafine concentration, and the 24-hour mean was selected as representative of the time scale of the synoptic meteorological systems. We did not change our averaging period to match the changing meteorology. Shortening the averaging period made the dew point parameter more noisy but did not change the overall result.

The time series of ultrafine concentration, dew point difference, and sea level pressure for a 15-day period during RITS 94 in the southern midlatitudes and Southern Ocean (45° to 65°S) is shown in Figure 9. During this period there were several transitions between high and low pressure areas and several frontal passages. The peaks in ultrafine concentration coincided with either high pressure or stabilizing atmospheric pressure after the passage of a low, trough, or frontal zone. The first four concentration peaks corresponded to decreasing dew point, i.e., negative values of $\bar{T}_d(6) - \bar{T}_d(24)$. The correspondence was not so clear after Julian Day 364 due to changing meteorological

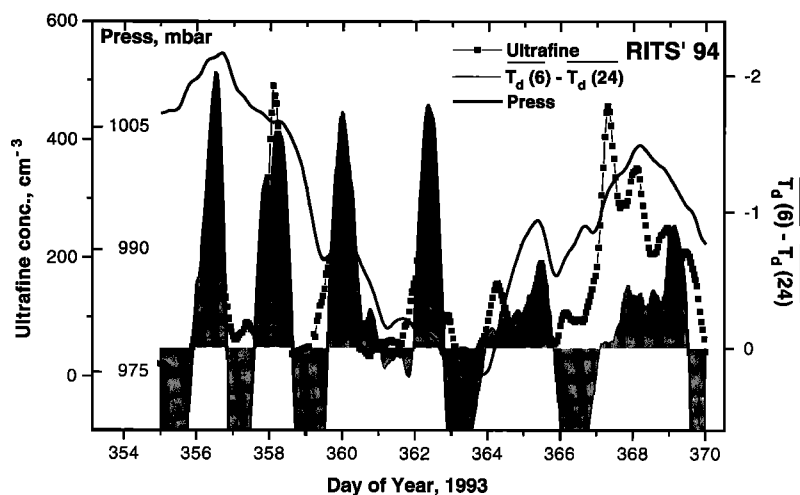


Figure 9. Ultrafine number concentration, $n(>3) - n(>14)$, cm^{-3} ; sea level pressure, millibars; and the difference between 6-hour and 24-hour running means of dew point temperature, $\overline{T_d}(6) - \overline{T_d}(24)$, during RITS 94.

scales from about 24 to 48 hours. We interpret this correspondence as evidence that the source of ultrafine particles in the MBL is subsidence and entrainment from the FT.

A similar analysis was made with ultrafine particle and ozone concentrations. The result was not inconsistent with the above analysis but was not so clear. An attempt to use vertical profiles from the rawinsonde data to construct conserved variable diagrams [Hegg *et al.*, 1992] of the atmosphere in the vicinity of the ship and to estimate mixing and entrainment was unsuccessful due to the rapid movement of the ship with respect to the weather systems.

One of many critical variables for the nucleation of new particles from condensable vapors such as H_2SO_4 is the surface area concentration of existing particles. If this concentration is low enough (i.e., <10 to $20 \mu\text{m}^2/\text{cm}^3$) new particle formation can be expected, based on model calculations and previous observations [Covert *et al.*, 1992; Gras, 1993; Raes, 1995]. If this concentration is high, particle production will be suppressed since most of the condensable vapors will condense on existing particles rather than nucleating new particles. As a consequence of this, a plot of ultrafine particle concentration versus particulate surface area should show an increase in ultrafine concentration with decreasing surface area when new particle production occurs in the MBL. Figure 10a shows such a scatter plot for RITS 94. There is clearly no inverse relationship in this data set. If there is a relationship, it is positive, that is, the ultrafine concentration was slightly correlated with the Aitken mode concentration, which contained a significant fraction of the submicrometric particulate surface area. Notably, seldom during any of the three cruises was the aerosol surface area low enough that new particle formation could be expected. Even at the lowest observed surface area concentrations, about $5 \mu\text{m}^2 \text{cm}^{-3}$, there were no concurrent occurrences of high particle concentrations in the ultrafine or Aitken size ranges. This is consistent with the model results of Raes [1995] in which MBL nucleation is suppressed by the entrainment of aerosol from the FT into the MBL. If lower surface area concentrations had been encountered over longer time periods, the expected inverse relation might have been observed.

A scatter plot of ultrafine particle concentration versus DMS concentration for RITS 94 is presented in Figure 10b. Although there were numerous occasions of very high DMS concentra-

tion, some of which extended over periods of many hours, there is no evidence of a direct correlation between DMS and ultrafine particle concentration for the data set as a whole or for any logical time- or location-based subset of the data. A similar data set [Andreae *et al.*, 1995], including measurements of DMS and condensation nuclei (CN), $n(>10 \text{ nm})$, in the tropical South

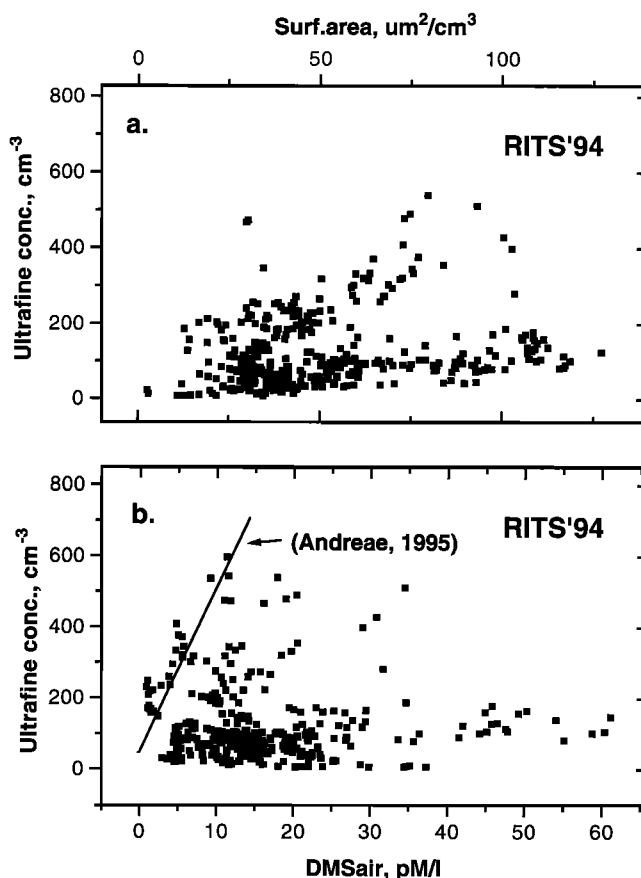


Figure 10. Ultrafine number concentration, $n(>3) - n(>14)$, cm^{-3} , versus: (a) particulate surface area, micrometers squared per cubic centimeter; and (b) dimethylsulfide concentration in air, DMS_a , pM/l . Data from RITS 94.

Atlantic, indicated a weak but statistically significant correlation between those parameters, from which a MBL source of new particles was inferred. The correlation line obtained by *Andreae et al.* [1995] is overlaid on Figure 10b for comparison. The major source of covariance in their data could be due to large, geographical-scale (1000-km) changes in CN and DMS as the cruise track passed from west to east through the South Atlantic high-pressure region with presumably relatively constant 1- to 2-day upwind conditions. These conditions of relatively long MBL residence times could have resulted in oxidation of DMS to condensable aerosol precursors. (Our data at similar latitudes, by contrast, were gathered on north-south cruise tracks passing through more changeable meteorological conditions.) However, an aerosol surface area of $40 \mu\text{m}^2/\text{cm}^3$ (consistent with the

number and volume data of *Andreae et al.* [1995] for the accumulation and sea salt modes) is high compared to that required for new particle formation according to prevalent models. Alternatively, the correlation obtained by *Andreae et al.* [1995] may have been due to growth of particles less than about 10 nm in diameter (mixed from the upper troposphere in the regions of stratocumulus and high DMS) into the size range sensed by their instrumentation. Three-dimensional trajectory analysis and MBL stability and mixing depth data to determine the potential for an upper tropospheric source were not presented by *Andreae et al.* [1995] but could have provided clues of such a source.

From our analysis of the relation between ultrafine concentration and particulate surface area and DMS, we conclude that

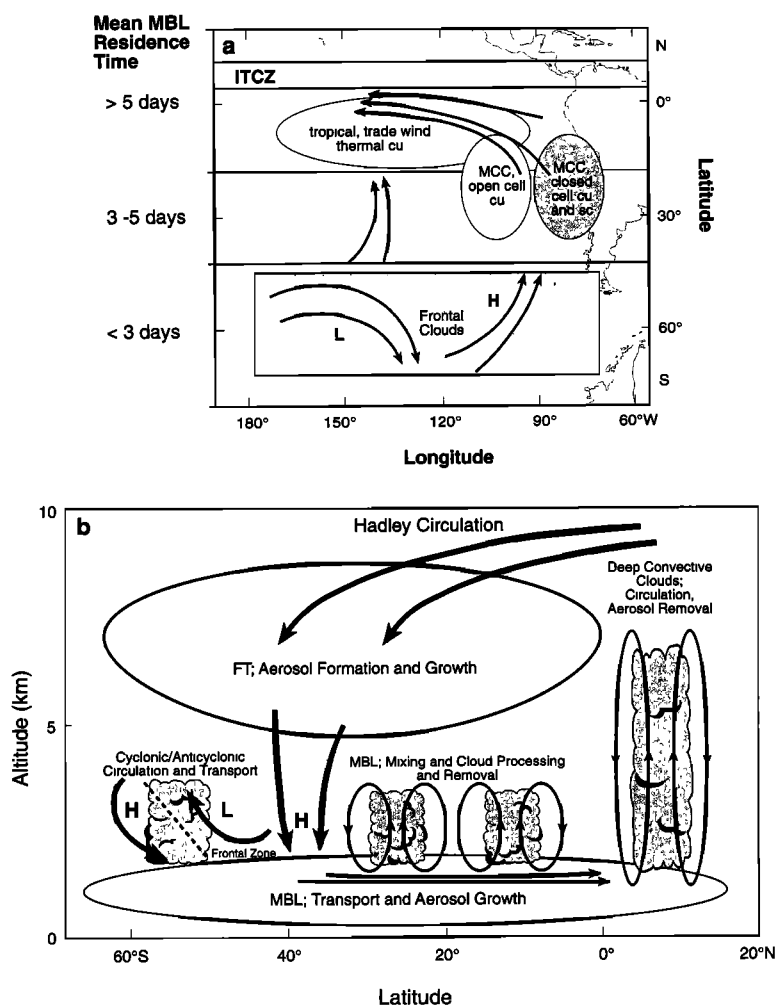


Figure 11. Schematic, horizontal, and vertical representation of sources, processing, and transport of aerosol in the MBL and FT of the mid-Pacific, which are consistent with surface observations of the MAGE and RITS cruises, observations aloft, general atmospheric circulation, and particle nucleation and growth models. (a) New particle formation occurs in outflow regions from clouds in the free troposphere associated with frontal or convective vertical motions. Transport of aerosols from the FT to the MBL occurs by regional-scale or mesoscale subsidence. Transport into and within the MBL occurs by convective mixing in the vertical and general circulation in the horizontal. Aerosol growth by vapor deposition occurs in all regions, but is most effective in the tropical MBL where gaseous precursor concentrations are high. Processing by clouds is effective in transferring the aerosol from the Aitken to the accumulation mode by deposition of vapors and heterogeneous oxidation of sulfur gases on or within cloud droplets. (b) Typical cloud fields and large-scale horizontal air motions in the MBL for the mid- and South Pacific portions of the cruises. Shaded regions indicate different generic cloud types (including cumulus, stratocumulus, and frontal clouds) and the associated types of circulation associated with their formation (thermal convection, open and closed mesoscale cellular convection, MCC, and frontal convection).

there was little new particle production in the part of the MBL that we observed and that most of the ultrafine and Aitken-sized particles came from the FT. The majority of the available sulfuric acid vapor from oxidation of DMS most likely condensed on existing particles to form new particulate mass and to increase the size of those particles rather than to form and grow new particles.

Integrating the above information, we present a schematic model representing the aerosol cycle in the southern hemisphere MBL (Figure 11). It is similar to that presented by Ito [1993] with an extension to more equatorial latitudes and it is consistent with the MBL data presented here, the FT data of Clarke [1993], and the models of Raes *et al.* [1993] and Raes [1995]. The model is confined to the southern hemisphere at this time because of the more variable data set observed in the northern hemisphere portion of our cruises. This variability was due to more complex weather systems during the seasons of the studies and the greater influence of continental and anthropogenic sources of aerosol in the northern hemisphere.

Considering the vertical representation first, we hypothesize that the main source of particles to the MBL is the FT, where new particles are formed by homogeneous binary (or higher-order) nucleation in the outflow regions of clouds, either in frontal zones of the midlatitudes or in convective cells in the tropics, as is depicted by the upward arrows in Figure 11a. New particle production is particularly likely in these regions [Raes *et al.*, 1993]. The surface area of preexisting aerosol is low as a result of scavenging of aerosols by cloud droplet nucleation and precipitation, temperatures are relatively low, relative humidity (RH) is relatively high, and DMS is transported efficiently from surface levels through the clouds due to its relative insolubility. New particles formed in this region grow by coagulation and condensation in the large-scale Hadley and Walker circulations. The evolution of aerosol in the FT has been modeled with an aerosol dynamics model [Raes *et al.*, 1993] and later as a self-preserving number distribution [Raes, 1995]. It is not expected, based on the self-preserving model, that particles will be able to grow to sizes much larger than the Aitken mode within reasonable residence times of 1 to 2 weeks for the FT.

This FT aerosol is eventually transported to the lower troposphere by regional and hemispheric-scale motions, where it may be brought directly to the surface by strong subsidence or mixed across the inversion at the top of the MBL. The broad downward arrows in Figure 11a depict this large-scale transport and subsidence as motion associated with Hadley cell or anticyclonic circulation. There is also subsidence on a smaller scale, associated with deep convective cells in the ITCZ and mesoscale cellular convection (MCC) [Agee, 1987] in the subtropics and midlatitudes, which may bring FT air to the surface. Although the regionally averaged motion in the ITCZ is clearly upward, on a smaller scale there are likely to be parcels of air in this region that move downward, as depicted by the single arrows in the region of the ITCZ. Where subsidence is not strong enough to penetrate through the temperature inversion at the top of the MBL to the surface, transport across the inversion may be limited and proceed more slowly with time through entrainment across the inversion in association with MCC and cumulus or stratocumulus clouds. The flux of Aitken particles to the MBL depends on the FT concentration and the entrainment rate; their relative size depends on aging processes in the FT.

The representation of horizontal transport in the MBL and qualitative general MBL residence times for the aerosol cycle are illustrated in Figure 11b. The schematic trajectories illustrate

the paths traveled by air masses in the MBL. The shaded areas represent the typical cloud types found in the regions [Agee, 1987; Warren *et al.*, 1988]. In the tropical and subtropical latitudes south of the ITCZ the back trajectories are E to ESE and have the longest residence time in the MBL, i.e., 5 days or more. Nearer the equator they are confined to the region of the tropics and subtropics which is dominated by trade wind flow and tropical cumulus. Farther south, the back trajectories originate in the region of closed cell cumulus and stratocumulus associated with MCC in the flow along the coast of South America and eventually in the region of open cell cumulus in MCC in the more central Pacific. (Open and closed cell classification refers to mesoscale organization in marine cloud structures described by E. M. Agee and may be related to the rate of entrainment into the MBL from the FT and the rate of cloud processing of marine aerosol.) South of about 30°S, the time and distance that the trajectories spend in the MBL are shorter and the influence of midlatitude circulation, especially subsidence in anticyclonic flow, is noticeable. South of about 40°S the residence time of air in the MBL is the shortest due to rapid motion of baroclinic disturbances in the westerly jet. The region is characterized by alternating short MBL trajectories (rapid subsidence) from the SW, and MBL trajectories from the NW that are longer, but generally with residence times of a few days or less.

Submicrometric aerosol particles in the MBL grow by homogeneous and heterogeneous mechanisms and are removed by cloud droplet nucleation and precipitation scavenging. Significant growth of Aitken mode particles from the FT by homogeneous oxidation or condensation mechanisms is limited. The majority of the particles in the accumulation mode are almost certainly produced by cloud processes that convert Aitken mode particles to significantly larger sizes in a single passage or multiple passages through a cloud [Hoppel, 1994]. Larger Aitken mode particles nucleate to form cloud droplets in which adsorbed gases oxidize to form more solute mass, which remains with the aerosol upon detrainment and evaporation of the cloud droplet. The relative concentration of the accumulation mode depends on the frequency of cloud processing and supersaturation in the clouds, that is, the number of Aitken mode particles nucleated (thus converted), and on the efficiency and frequency of precipitation scavenging. The relative size of the accumulation mode depends on cloud droplet size, the number of cloud passes, and the available concentration of gas phase species, for example, SO₂ and NH₃. A more quantitative treatment of these processes requires the use of MBL and cloud physics models with input conditions including observations such as these and satellite cloud analyses merged with air mass trajectory analysis.

Conclusions

The aerosol number-size distribution has modal features which are similar throughout large latitudinal regions of the South Pacific MBL and which depend on the MBL and FT sources of particles and their precursor gases. Similar features are present in the North Pacific, but there the patterns are influenced by continental and anthropogenic sources of aerosol from North America as well as by marine sources. Changes in the modal features occur over regional scales and mesoscales. These changes are consistent with meteorological transport and aerosol transformation processes operating on those scales. Conditions of strong subsidence and entrainment from the FT produce an aerosol dominated by particles in the Aitken mode,

about 25 to 60 nm or smaller in diameter. Residence time in the MBL of a few days or more results in a significantly modified aerosol which is bimodal with roughly equal contributions to the total number from the Aitken mode and the accumulation mode (between 150 and 200 nm diameter). In our extensive data set there was no indication of rapid new particle formation in the MBL; particle source seemed to be dominated by entrainment from the FT. However, the major source of new particle mass, resulting from a combination of vapor condensation and cloud processes, was most likely the MBL. The data set reported here has enabled the description of the particle number distribution and its variability with latitude and meteorology, which is needed to improve models of aerosols in the MBL.

Acknowledgments. This research was supported by NSF Division of Atmospheric Chemistry grant ATM 931112, the Aerosol Component of the NOAA Climate and Global Change Program, and the NASA Mission to Planet Earth Science Division. This is JISAO contribution 315 and NOAA PMEL contribution 1629. We thank the officers and crew of the University of Southern California RV *Vickers* and NOAA RV *Surveyor* for their assistance. This research is a contribution to the International Global Atmospheric Chemistry (IGAC) Core Project of the International Geosphere-Biosphere Programme (IGBP).

References

- Agee, E. M., Mesoscale cellular convection over the oceans, *Dyn. Atmos. Oceans*, **10**, 317–341, 1987.
- Andreae, M. O., W. Elbert, and S. J. de Mora, Biogenic sulfur emissions and aerosol over the tropical South Atlantic, *J. Geophys. Res.*, **100**, 11,335–11,356, 1995.
- Bates, T. S., K. C. Kelly, and J. E. Johnson, Concentrations and fluxes of dissolved biogenic gases (DMS, CH₄, CO, CO₂) in the equatorial Pacific during the SAGA 3 experiment, *J. Geophys. Res.*, **98**, 16,969–16,978, 1993.
- Clarke, A., Atmospheric nuclei in the Pacific midtroposphere: Their nature, concentration and evolution, *J. Geophys. Res.*, **98**, 20,633–20,647, 1993.
- Covert, D. S., V. N. Kapustin, P. K. Quinn, and T. S. Bates, New particle formation in the marine boundary layer, *J. Geophys. Res.*, **97**, 20,581–20,589, 1992.
- Draxler, R. R., Hybrid Single-Particle Lagrangian Integrated Trajectories (HY-SPLIT): Version 3.0, Users guide and model description, NOAA ARL, Silver Spring, Md., 1992.
- Gras, J. L., Condensation nucleus size distribution at Mawson, Antarctica: Microphysics and chemistry, *Atmos. Environ.*, **27A**, 1427–1434, 1993.
- Hegg, D. A., D. S. Covert, and V. N. Kapustin, Modeling a case of particle nucleation in the marine boundary layer, *J. Geophys. Res.*, **97**, 9851–9857, 1992.
- Hoppel, W. A., and G. M. Frick, Submicron aerosol size distributions measured over the tropical and south Pacific, *Atmos. Environ.*, **24A**, 645–659, 1990.
- Hoppel, W. A., G. M. Frick, J. W. Fitzgerald, and R. E. Larson, Marine boundary layer measurements of new particle formation and the effect which non-precipitating clouds have on the aerosol size distribution, *J. Geophys. Res.*, **99**, 14,443–14,459, 1994.
- Ito, T., Antarctic submicron aerosols and long-range transport of pollutants, *Ambio*, **18**, 34–41, 1989.
- Ito, T., Size distribution of Antarctic submicron aerosols, *Tellus*, **45B**, 145–159, 1993.
- Kerminen, V. M., and A. S. Wexler, Enhanced formation and development of sulfate particles due to marine boundary layer circulation, *J. Geophys. Res.*, in press, 1995.
- Quinn, P. K., D. S. Covert, T. S. Bates, V. N. Kapustin, D. C. Ramsey-Bell, and L. M. McInnes, Dimethylsulfide/cloud condensation nuclei/climate system: Relevant size-resolved measurements of the chemical and physical properties of atmospheric aerosol particles, *J. Geophys. Res.*, **98**, 10,411–10,427, 1993.
- Quinn, P. K., T. S. Bates, V. N. Kapustin, and D. S. Covert, Chemical and optical properties of marine boundary layer aerosol particles of the mid-Pacific in relation to sources and meteorological transport, *J. Geophys. Res.*, accepted, 1995.
- Raes, F., Entrainment of free tropospheric aerosols as a regulating mechanism for cloud condensation nuclei in the remote marine boundary layer, *J. Geophys. Res.*, in press, 1995.
- Raes, F., R. Van Dingenen, J. Wilson, and A. Saltelli, Cloud condensation nuclei from dimethylsulphide in the natural marine boundary layer: Remote vs in-situ production, in *Dimethylsulphide – Oceans, Atmosphere and Climate*, edited by G. Restelli and G. Angeletti, pp. 311–322, Kluwer Academic, Norwell, Mass., 1993.
- Russell, L. M., S. N. Pandis, and J. H. Seinfeld, Aerosol production and growth in the marine boundary layer, *J. Geophys. Res.*, **99**, 20,989–21,003, 1994.
- Salinger, M. J., R. E. Basher, B. B. Fitzharris, J. E. Hay, P. D. Jones, J. P. Macveigh, and I. Schmidley-Lelue, Climate trends in the South-west Pacific, *Int. J. Climatology*, **15**, 285–302, 1995.
- Warren, S. G., C. J. Hahn, J. London, R. M. Chervin, and R. L. Jenne, Global distribution of total cloud cover and cloud type amounts over the ocean, NCAR Tech. Memo., Natl. Cent. for Atmos. Res., Boulder, Colo., 1988.
- Wendland, W. M., and N. S. McDonald, Southern hemisphere airstream: Climatology, *Mon. Weather Rev.*, **114**, 88–94, 1986.
- Yvon, S. A., E. S. Saltzman, D. J. Cooper, T. S. Bates, and A. M. Thompson, Atmospheric dimethylsulfide cycling at a tropical South Pacific station (12°S, 135°W): A comparison of field and model results, *J. Geophys. Res.*, in press, 1995.

T. S. Bates and P. K. Quinn, NOAA, Pacific Marine Environmental Lab, Seattle, WA 98115. (e-mail: bates@pmel.noaa.gov; quinn@pmel.noaa.gov)

D. S. Covert, Department of Atmospheric Sciences, University of Washington, Seattle, WA 98195. (e-mail: dcovert@u.washington.edu)

V. N. Kapustin, Joint Institute for Study of Atmosphere and Ocean, University of Washington, Seattle, WA 98195 (e-mail: kapustin@pmel.noaa.gov)

(Received March 11, 1995; revised October 3, 1995; accepted October 4, 1995.)